



Dislocation density dependent photorefractive effect in (001)-cut GaAs

K. Jarasiunas, J. Vaitkus, Philippe Delaye, Gérald Roosen

► To cite this version:

K. Jarasiunas, J. Vaitkus, Philippe Delaye, Gérald Roosen. Dislocation density dependent photorefractive effect in (001)-cut GaAs. Optics Letters, 1994, 19 (23), pp.1946-1948. hal-00673561

HAL Id: hal-00673561

<https://hal-iogs.archives-ouvertes.fr/hal-00673561>

Submitted on 24 Feb 2012

HAL is a multi-disciplinary open access archive for the deposit and dissemination of scientific research documents, whether they are published or not. The documents may come from teaching and research institutions in France or abroad, or from public or private research centers.

L'archive ouverte pluridisciplinaire **HAL**, est destinée au dépôt et à la diffusion de documents scientifiques de niveau recherche, publiés ou non, émanant des établissements d'enseignement et de recherche français ou étrangers, des laboratoires publics ou privés.

Dislocation density-dependent photorefractive effect in (001)-cut GaAs

K. Jarasiunas and J. Vaitkus

Institute of Material Science and Applied Research, Vilnius University, Saulėtekio Avenue 9-3, Vilnius 2054, Lithuania

P. Delaye and G. Roosen

Institut d'Optique Théorique et Appliquée, Unité de Recherche Associée 14 au Centre National de la Recherche Scientifique, Bât. 503, Centre Scientifique d'Orsay, B.P. 147, 91403 Orsay Cedex, France

Received April 19, 1994

We present studies of the photorefractive effect in nonphotorefractive orientations of liquid-encapsulated Czochralski-grown GaAs crystals. Picosecond diffraction experiments conducted in different samples show that a forbidden photorefractive signal correlates well with dislocation density, which points out that the effect arises from strain fields and growth defects.

Degenerate four-wave mixing in semiconductors reveals many different physical mechanisms. In photorefractive (PR) semiconductors, two mechanisms of refractive-index modulation coexist at short-pulse excitation: an intrinsic local one, based on nonequilibrium carriers, and a second one, of PR origin, based on internal space-charge electric fields that arise from fast-carrier redistribution. Free-carrier (FC) nonlinearity is isotropic, and for frequencies far from the direct band gap it is described by the Drude-Lorentz model.¹ For the PR mechanism the index modulation seen by a probe beam depends on the beam's polarization and on the orientation of the crystal principal axes with respect to grating vector K_g :

$$\Delta n_{\text{PR}} = -\frac{n_0^3 r_{\text{eff}} E_{\text{sc}}}{2}, \quad (1)$$

where $r_{\text{eff}} = e_i [R \ k_g] e_d$ is the effective electro-optic coefficient, R is the electro-optic tensor, $e_{i,d}$ are the polarization vectors of incident and diffracted waves, k_g is the unit grating vector, n_0 is the linear refractive index, and E_{sc} is the space-charge electric field. For crystals with $43m$ symmetry, the anisotropy of light diffraction on PR grating was analyzed.² In the common PR crystal cut (i.e., faces along crystallographic directions $[110]$, $[\bar{1}10]$, and $[001]$) and for K_g along $[110]$, a rotation of polarization of diffracted beam takes place (a phenomenon known as anisotropic diffraction). This peculiarity was used to separate contributions of the PR grating from the contributions of the much stronger but isotropic FC grating at picosecond pulse excitation.³⁻⁵

Recent investigations of PR gratings in GaAs crystals have revealed an unexpected diffracted signal with a rotated polarization for a grating whose orientation is $K_g // [001]$.⁵ This cannot be explained by any conventional electro-optic mechanism, which predicts $r_{\text{eff}} = 0$ for anisotropic diffraction in this geometry.² This phenomenon was attributed to internal strains and electric fields around charged dislocations, which may break the crystal symmetry

and create new components in the electro-optic tensor. Unlike in GaAs, no anisotropic diffracted signal has been observed on gratings oriented along $[001]$ in PR-cut vanadium-doped CdTe crystals grown by the Bridgman technique. Because the latter growth technique gives a very low density of dislocations, this observation also supports our hypothesis that local strains and electric fields at macroscopic defects are what cause a nonzero effective electro-optic coefficient. Recently observed PR effects in strained centrosymmetric KTN and KTLN crystals also were attributed to the presence of growth-induced strain.⁶

In this Letter we extend our studies on the origin of this novel effect, which we believed to be dependent on dislocation density. Samples of liquid-encapsulated Czochralski-grown GaAs with different dislocation densities and specific nonphotorefractive orientations are investigated. Degenerate four-wave mixing experiments are performed with the setup described in our previous work.⁵ We use a YAG laser emitting a 28-ps-duration pulse with energy density up to 10 mJ cm^{-2} at a $1.06-\mu\text{m}$ wavelength. Two *s*-polarized beams of equal intensity record a grating with period $\Lambda = 1.8 \mu\text{m}$. The decay of PR and FC gratings is monitored by a delayed *s*-polarized or *p*-polarized probe beam and a polarization-sensitive readout system.

PR and FC picosecond gratings are studied in four GaAs crystals. The first sample (#1), an undoped semi-insulating GaAs crystal ($\rho = 5 \times 10^7 \Omega \text{ cm}$, dislocation density $N_D = 10^5 \text{ cm}^{-2}$, thickness $d = 1.5 \text{ mm}$), is cut in a typical photorefractive way. Transient gratings in this sample are studied in two orientations ($K_g // [110]$ and $K_g // [001]$), with light beams propagating along direction $[110]$. In both cases the *p*-diffracted component of the *s*-polarized probe beam is attributed to the PR grating contribution, while the nonrotated component of the *p*-polarized probe gives the strength and decay of the FC grating.

The next three samples are cut along plane (001), i.e., an orientation in which electro-optic theory predicts a zero PR signal for beams propagating along direction [001]. Sample #2 is a semi-insulating In-alloyed wafer ($\rho = 5 \times 10^6 \Omega \text{ cm}$, $N_D = 3 \times 10^4 \text{ cm}^{-2}$, $d = 1.1 \text{ mm}$). Samples #3 and #4 are commercial (001)-grown GaAs wafers: a semi-insulating one ($\rho = 5 \times 10^7\text{--}10^8 \Omega \text{ cm}$, $N_D = 4 \times 10^4 \text{ cm}^{-2}$, $d = 0.5 \text{ mm}$) and one heavily doped with silicon up to the free-electron concentration $N = 10^{18} \text{ cm}^{-3}$ ($\rho = 10^{-4} \Omega \text{ cm}$, $N_D = 2 \times 10^3 \text{ cm}^{-2}$, $d = 0.5 \text{ mm}$). The dislocation density in the latter sample is rather low because of strong doping with a shallow impurity.⁷

We compare the diffraction characteristics of semi-insulating GaAs (sample #1) in two different orientations of the grating vector ($K_g // [110]$ and $K_g // [001]$ axes) to analyze the origin of the observed effect.⁵ Dependencies of the diffracted beam energy I_1 versus excitation energy density I_0 (so-called exposure characteristics) and decay characteristics of the gratings (I_1 versus probe beam delay time Δt) are measured.

At short-pulse excitation, electric fields of two origins are created in photorefractive GaAs crystals: a space-charge field E_1 between ionized EL2 donors and electrons at monopolar carrier generation and a Dember field E_2 between electrons and holes.⁸ The transfer from a monopolar (E_1) to a bipolar (E_2) regime is seen in both decay and exposure characteristics. The decay of the first component is governed by dielectric relaxation, while E_2 is erased by ambipolar diffusion. The ratio E_1/E_2 varies with excitation and time. An indication of a grating erasure by diffusion is given by a fast component whose time constant decreases with excitation and reaches its ambipolar limit

$$\tau_a = \frac{e}{K_g^2 k_B T} \frac{n/\mu_p + p/\mu_n}{n + p} = 43 \text{ ps}$$

at high excitations ($n = p$)⁵ (n and p are the free-electron and hole densities). For example, for $K_g // [110]$ we find the decay time of the PR grating $\tau_{\text{PR}} = 65 \text{ ps}$ at $I_0 = 4 \text{ mJ cm}^{-2}$ (Fig. 1, curve 2). Similar behavior is observed for the unexpected signal resulting from anisotropic diffraction on the grating recorded with $K_g // [001]$, as illustrated in Fig. 1, curve 1.

The transfer from the slow field component E_1 to the fast one E_2 with increasing excitation also is revealed as a change in the power law dependence $I_1 = A I_0^\gamma$.⁵ For FC gratings the slope $\gamma = \Delta[\log(I_1)]/\Delta[\log(I_0)]$ decreases from $\gamma = 4\text{--}5$ to $\gamma = 3$, as found experimentally.^{4,5} For PR gratings the decrease in γ value always is more pronounced (from $\gamma_1 = 4\text{--}5$ to $\gamma_2 = 2\text{--}2.5$; see Fig. 2). This is because the decrease in the FC grating is compensated by a nonlinear increase of carrier concentration owing to two-photon absorption of light, whereas the PR effect, based on carrier transport, depends only on relative modulations of gratings. Slopes of exposure characteristics (Fig. 2) show identical behavior of anisotropic signals detected in both grating orientations.

All these similarities in exposure and temporal features confirm that the physical origin of the diffracted signal observed in orientation $K_g // [001]$ is the same as in $K_g // [110]$, i.e., of photorefractive origin.

In the following, we compare the strengths of the diffracted PR signals at a fixed value of $I_0 = 2.5 \text{ mJ cm}^{-2}$. The absolute value of $I_{1\text{PR}}$ is twice as large in the geometry $K_g // [001]$ (see Fig. 2). A similar increase in diffraction is observed for FC gratings. We also measure a stronger absorption of *s*-polarized beams⁹ (both recording and probe) in the orientation $K_g // [001]$. This increased absorption leads to more-pronounced increases of diffracted signals because of their relationship, which explains the above observation. The ratio of diffracted beam intensities is equal to $S_{(110)} = I_{1\text{PR}}/I_{1\text{FC}} = (1.6 \pm 0.2)\%$ in orienta-

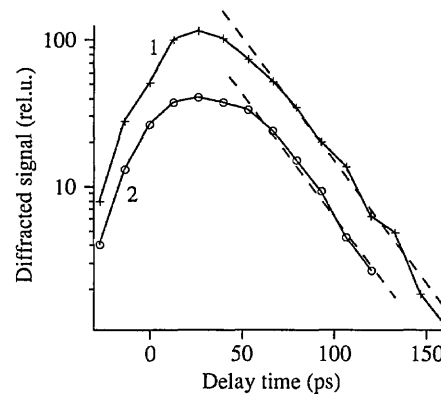


Fig. 1. PR grating dynamics at different crystal orientations and excitation levels of undoped GaAs sample #1: curve 1, $K_g // [001]$ at $I_0 = 3.5 \text{ mJ cm}^{-2}$; curve 2, $K_g // [110]$ at $I_0 = 4 \text{ mJ cm}^{-2}$. The dashed lines represent the decay time constant with a value of $\tau_{\text{PR}} = 65 \text{ ps}$. Zero delay time corresponds to coinciding probe and pump beams.

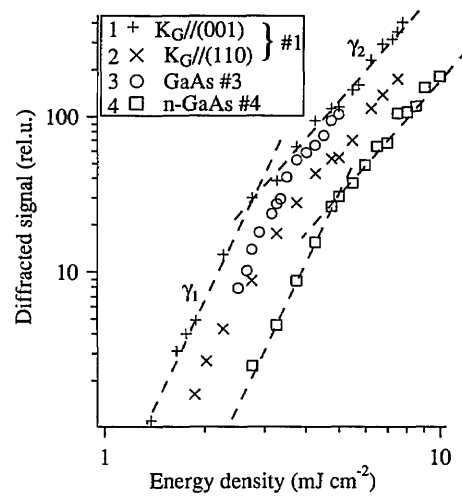


Fig. 2. Exposure characteristics of light diffraction on photorefractive gratings with period $\Lambda = 1.8 \mu\text{m}$ in differently cut and oriented GaAs crystals: light propagates along the $[110]$ axis and $K_g // [001]$ (curve 1) or $K_g // [110]$ (curve 2); light propagates along the $[001]$ axis in semi-insulating undoped (curve 3) and heavily doped (curve 4) GaAs crystals. The probe-beam delay time is 26 ps. The dashed lines indicate the slopes of the exposure characteristics (γ_1, γ_2).

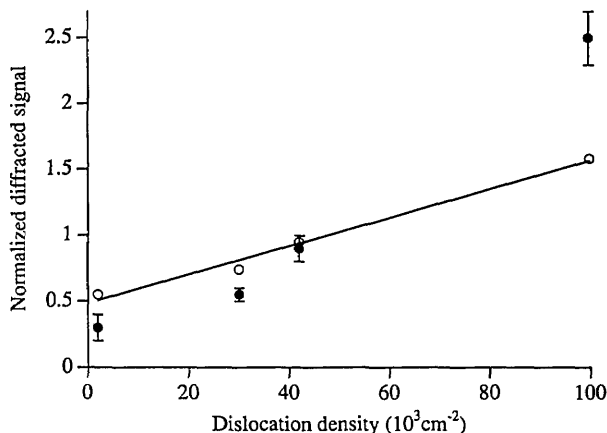


Fig. 3. Dependence of the ratio $S = I_{1\text{PR}}/I_{1\text{FC}}$ versus dislocation density N_D in liquid-encapsulated Czochralski-grown GaAs crystals with experimental points shown as filled circles. The straight line is a linear regression of the square root of S (open circles).

tion $K_g // [110]$ and $S_{(001)} = 2.3\text{--}2.7\%$ for orientation $K_g // [001]$.

We also will use this procedure of normalization of $I_{1\text{PR}}$ to $I_{1\text{FC}}$ in the following analysis for comparison of the strengths of the PR effect in (001)-cut samples with different absorption coefficients and thicknesses.

Even though $r_{\text{eff}} = 0$ for beams propagating along [001], time-resolved measurements of carrier dynamics in In-alloyed sample #2 also show the existence of an anisotropic diffracted signal that is created at excitations as low as 1 mJ cm^{-2} . At an excitation level of 2.5 mJ cm^{-2} this new PR signal is $I_{1\text{PR}} = 5\text{--}6 \text{ a.u.}$, and the FC signal is $I_{1\text{FC}} = 1000 \text{ a.u.}$, leading to a ratio $S = 0.5\text{--}0.6\%$ for this sample. The same anisotropic diffraction is observed in the undoped semi-insulating sample #3. A value of $S = 0.8\text{--}1\%$ is estimated at $I_0 = 2.5 \text{ mJ cm}^{-2}$. For sample #4, heavily doped n -GaAs, we also observe a p -diffracted component of an s -polarized probe beam, but the diffracted signal strength is smaller than those in semi-insulating samples. A value $S = 0.3\%$ at $I_0 = 2.5 \text{ mJ cm}^{-2}$ is obtained. The similarity in behavior revealed in exposure characteristics (Fig. 2) points out a common origin of this anisotropic diffraction.

The results are summarized in Fig. 3. They clearly show the decrease of the PR signal in non-photorefractive geometry with decreasing dislocation density. The ratio of $I_{1\text{PR}}/I_{1\text{FC}}$ is the square of the ratio of induced changes of refractive index that are due to the electro-optic effect and to the FC grating:

$$S = \frac{I_{1\text{PR}}}{I_{1\text{FC}}} = \frac{(\pi \Delta n_{\text{PR}} d / \lambda)^2}{(\pi \Delta n_{\text{FC}} d / \lambda)^2} = \left(\frac{\Delta n_{\text{PR}}}{\Delta n_{\text{FC}}} \right)^2. \quad (2)$$

The PR index modulation is $\Delta n_{\text{PR}} = -(r_{\text{eff}}^* E_{\text{SC}} n_0^3)/2$ (where r_{eff}^* is the effective electro-optic coefficient in the presence of dislocations). PR index modulation

owing to free carriers is $\Delta n_{\text{FC}} = -n_{\text{eh}} \Delta n$, where n_{eh} is the refractive-index change that is due to one electron-hole pair, according to the Drude model,¹ and Δn is the modulated population of free electrons. The excitation-dependent values are E_{SC} and Δn only, and, consequently, we have $S \propto [r_{\text{eff}}^*(E_{\text{SC}}/\Delta n)]^2$. The experiments have shown that, in all samples and orientations used, slopes γ of PR and FC gratings are the same (as illustrated in Fig. 2 for PR signals). This indicates that space-charge fields and carrier concentrations are coupled and would give a constant value of $E_{\text{SC}}/\Delta n$. Thus \sqrt{S} varies linearly with r_{eff}^* . An experimentally found variation of S with dislocation density is shown in Fig. 3 (filled circles). From these values we plot the square root of ratio S (Fig. 3, open circles), which shows a linear dependence of r_{eff}^* versus dislocation density. The correlation between anisotropic diffraction strength and dislocation density strongly supports the hypothesis that dislocations are responsible for the PR effect in (001)-cut GaAs samples.

The presence of charged dislocations creates piezoelectric effects and dichroism of optical absorption, which can be responsible for the creation of new coefficients of the electro-optic tensor. Further studies of optical nonlinearities, using nanosecond duration laser pulses and different wavelengths, will allow us to reach a better understanding of mechanisms involved in dislocation-governed refractive-index modulation.

K. Jarasiunas acknowledges many valuable discussions with Jurgis Storasta and financial support by International Science Foundation long-term grant LA9000.

References

1. R. K. Jain and M. B. Klein, in *Optical Phase Conjugation*, R. A. Fisher, ed. (Academic, New York, 1983), p. 307.
2. J. C. Fabre, J. M. C. Jonathan, and G. Roosen, Opt. Commun. **65**, 257 (1988).
3. W. A. Schroeder, T. S. Stark, M. D. Dawson, T. F. Bogess, A. L. Smirl, and G. C. Valley, Opt. Lett. **16**, 159 (1991).
4. K. Jarasiunas, P. Delaye, J. C. Launay, and G. Roosen, Opt. Commun. **93**, 59 (1992).
5. K. Jarasiunas, P. Delaye, and G. Roosen, Phys. Status Solidi B **175**, 445 (1993).
6. R. Hofmeister, A. Yariv, S. Yagi, and A. Agranat, Phys. Rev. Lett. **69**, 1459 (1992); erratum **72**, 435 (1994).
7. R. N. Thomas, S. McGuigan, G. W. Eldridge, and D. L. Barret, Proc. IEEE **76**, 778 (1988).
8. A. E. Smirl, G. C. Valley, K. M. Bohnert, and T. F. Bogess, IEEE J. Quantum Electron. **24**, 289 (1988).
9. Absorption of linearly polarized light in media with oriented dislocations depends on the orientation of the electric vector of the light beam; see L. I. Stephanovitch and E. P. Feldman, Sov. Phys. Solid State **27**, 725 (1985); D. Vignaud and J. L. Farvacque, J. Appl. Phys. **65**, 1261 (1989).